ACS Catalysis

Research Article

Cite This: ACS Catal. 2018, 8, 1097−1103

pubs.acs.org/acscatalysis

Quaternary Alkyl Ammonium Salt-Catalyzed Transformation of Glycidol to Glycidyl Esters by Transesterification of Methyl Esters

Shinji Tanaka,*[,†] Takuya Nakashima,[†] Toshie Maeda,[†] Manussada Ratanasak,[‡] Jun-ya Hasegawa,*[,‡] Yoshihiro Kon,[†] Masanori Tamura,[†] and Kazuhiko Sato*[,†]

[†]Interdisciplinary Research Center for Catalytic Chemistry, National Institute of Advanced Industrial Science and Technology, Central 5, 1-1-1 Higashi, Tsukuba, Ibaraki 305-8565, Japan

[‡]Institute for Catalysis, Hokkaido University, Kita 21, Nishi 10, Kita-ku, Sapporo 001-0021, Japan

Supporting Information

ABSTRACT: Catalytic transformation of glycidol while maintaining its epoxide moiety intact is challenging because the terminal epoxide that interacts with the hydroxyl group via a hydrogen bond is labile for the ring-opening reaction. We found that a quaternary alkyl ammonium salt catalyzes the selective transformation of glycidol to glycidyl esters by transesterification of methyl esters. The developed method can be applied to the synthesis of multiglycidyl esters, which are valuable epoxy resin monomers. Mechanistic studies revealed the formation of a binding complex of glycidol and quaternary alkyl ammonium salt in a nonpolar solvent and the generation of the alkoxide anion as a catalyst through the ring-opening reaction of the epoxide. Computational studies of the reaction mechanism indicated that the alkoxide anion derived from glycidol tends to abstract the proton of another glycidol rather than work as a nucleophile, initiating the catalytic transesterification. Payne rearrangement of the deprotonated glycidol, which produces a destabilized base that promotes nonselective reactions, is energetically unfavorable due to the double hydrogen bond between the anion and diol. The minimal interaction between the quaternary alkyl ammonium cation and the epoxide moiety inhibited the random ring-opening pathway leading to polymerization.

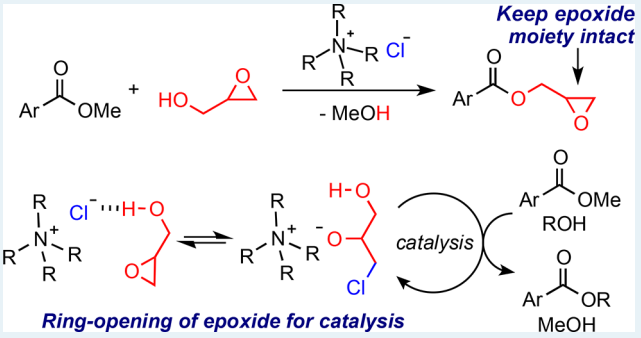

KEYWORDS: *organocatalyst, quaternary ammonium salt, glycidol, glycidyl ester, transesterification*

INTRODUCTION

Glycidol has attracted heightened interest due to its peculiar structure and reactivity, derived from the proximal accumulation of an epoxide and a hydroxyl group.[1−6] The development of glycidol as a feedstock for various fine chemicals is considered an important challenge[7] because recent studies suggested that glycidol can potentially be produced from glycerol and its derivatives.[8] Both acids and bases catalyze the transformation of glycidol (Scheme 1). Acid catalysts activate the epoxide moiety and convert it to various functional alcohols, including chiral alcohols, by the ring-opening reaction;[9] at the same time, base catalysts induce the ring-opening polymerization that results in the formation of hyperbranched polymers.[10−16] Another application of glycidol involves a transformation that keeps its epoxide intact, serving as an alternative method for the production of glycidyl compounds, which are valuable monomers for functional epoxy resins (Scheme 1).[17,18] The labile terminal epoxide moiety interacts with the hydroxy group via intramolecuar[14] and intermolecular hydrogen bonds,[19] however, thus hampering such selective transformations,[20] except for reactions with highly reactive substrates.[6,21,22] A strategy for activating glycidol by a catalyst that is neither an acid nor a base is therefore required.

Scheme 1. Catalytic Transformation of Glycidol

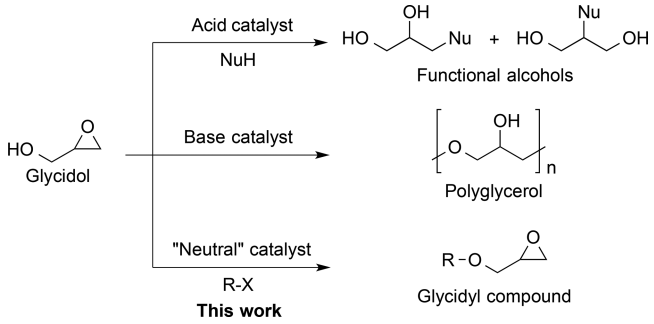

Glycidyl esters are an attractive target compound that can be prepared from glycidol because they are useful monomers of epoxy resins with high insulating properties.[17] Glycidyl esters

Received: September 26, 2017
Revised: December 3, 2017

DOI: 10.1021/acscatal.7b03303
ACS Catal. 2018, 8, 1097−1103

are conventionally synthesized by an epichlorohydrin process, in which a chlorine atom of epichlorohydrin is replaced by carboxylate and an equimolar amount of salt is generated as waste.[17,23] One issue with this process is the side reactions that generate organochlorine compounds as byproducts, because contamination by these byproducts negatively affects the performance of the epoxy resin. Furthermore, the recent use of halide compounds as commodity chemicals has been somewhat restricted due to their potential toxicity.[24] Transesterification of methyl esters with glycidol would generate glycidyl esters in a more environmentally benign way than the conventional process. Current catalysts, however, are limited to toxic salts such as Tl salts,[25] metal cyanide,[26,27] and selenocyanide,[26] presumably because common acid catalysts are not suitable for transesterification.[28−30]

To develop a method in which glycidol acts as a nucleophile during transesterification, we assumed that a neutral organocatalyst would be reasonable to mildly activate a molecule that is both acid- and base-sensitive. Organic salts having a distributed cation charge with a less basic anion would separate glycidol as a monomer form from the dimer structure in solution[1] and enhance the nucleophilic nature under mild conditions. Here we found that a simple quaternary alkyl ammonium salt facilitates the transesterification of methyl esters with glycidol, affording glycidyl esters. The mechanism of activation of glycidol by a quaternary alkyl ammonium salt during the catalytic cycle was elaborated by spectroscopic analysis as well as computational studies.

RESULTS AND DISCUSSION

Transesterification of methyl benzoate (**1a**) with 1.0 equiv of glycidol (**2**) in hexane at reflux temperature (69 °C) did not proceed at all without the catalyst (Figure 1, entry 1). Glycidyl

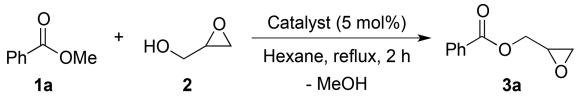

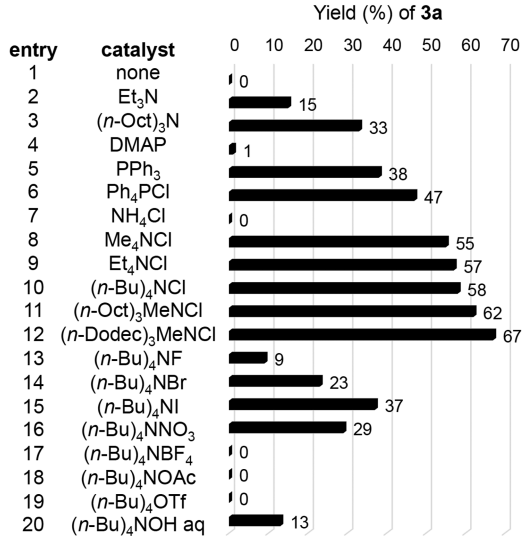

Figure 1. Catalytic transesterification of **1a** with **2**. Reaction conditions: **1a** (1.0 mmol), **2** (1.0 mmol), catalyst (0.050 mmol), hexane (0.5 mL), at reflux temperature (69 °C) for 2 h. Yields are determined by ^{1}H NMR using biphenyl as internal standard.

benzoate (**3a**) was obtained in low yields in the presence of bases such as Et_3N, $(n\text{-Oct})_3N$, DMAP, and PPh_3 (Figure 1, entries 2−5). Quaternary onium salts facilitated the reaction (Figure 1, entries 6, 8−12), and interestingly, the use of quaternary alkyl ammonium chlorides with longer alkyl chains gave higher yields of **3a**, while that of NH_4Cl resulted in 0% yield (Figure 1, entries 7−12). Screening of counteranions of $(n\text{-Bu})_4N^+$ salts indicated that Cl^- was optimal (Figure 1, entry 10), and other halogen anions, nitrate, and hydroxide also acted as catalysts in this reaction (Figure 1, entries 13−20).

Upon optimizing the catalytic conditions,[31] we evaluated methyl esters (Table 1). 4-Substituted phenyl glycidyl esters

Table 1. Scope of Substrates[a]

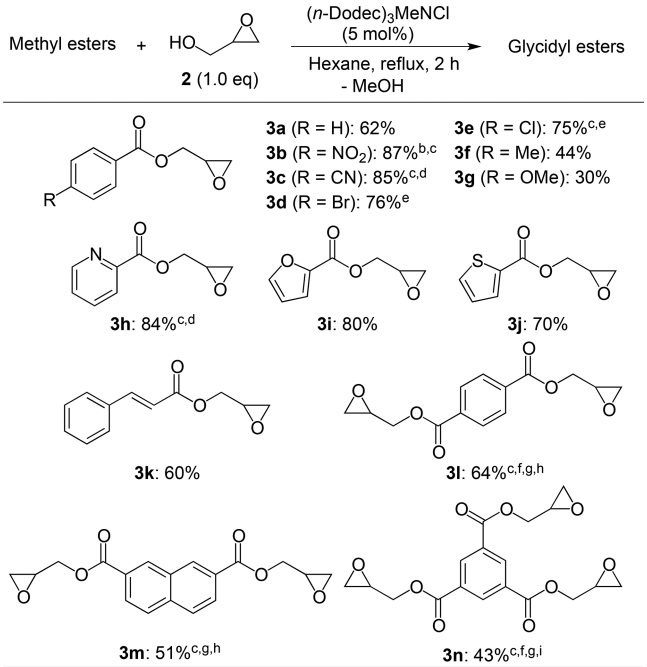

[a]Reaction conditions: methyl ester (1.0 mmol), **2** (1.0−3.0 mmol), catalyst (0.0010−0.050 mmol), hexane (0.5 mL), at reflux temperature (69 °C) for 2−3 h. Yields of isolated products are shown. [b]0.1 mol % of catalyst. [c]3 h. [d]1 mol % of catalyst. [e]2.5 mol % of catalyst. [f]0.5 mol % of catalyst. [g]Hexane (0.5 mL) + toluene (0.25 mL) was used as solvent. [h]2.0 equiv of **2**. [i]3.0 equiv of **2**.

such as glycidyl 4-nitrobenzoate (**3b**), glycidyl 4-cyanobenzoate (**3c**), glycidyl 4-bromobenzoate (**3d**), and glycidyl 4-chlorobenzoate (**3e**) were obtained in 75%−87% yields. Yields of esters with an electron-donating group in the aryl moiety, such as glycidyl 4-tolylate (**3f**) and glycidyl 4-anisylate (**3g**), however, were relatively low. Esters bearing heteroaromatic rings, such as glycidyl 2-pyridylate (**3h**), glycidyl 2-furylate (**3i**), glycidyl 2-thienylate (**3j**), and an alkenyl part, glycidyl cinnamate (**3k**) , were also prepared in moderate to high yields in the presence of a catalytic amount of $(n\text{-Dodec})_3$MeNCl (Dodec = $C_{12}H_{25}$). Moreover, substrates bearing more than two methyl ester moieties were converted to multiglycidyl compounds using $(n\text{-Dodec})_3$MeNCl and **2**; diglycidyl terephthalate (**3l**), diglycidyl 2,7-naphthalenedicarboxylate (**3m**), and triglycidyl 1,3,5-benzenetricarboxylate (**3n**) were isolated in 43%−64% yields. Notably, those multiglycidyl esters are useful monomers for functional epoxy resins, and are conventionally prepared from carboxylic acids and epichlorohydrin.[17,23] Alternatively, we successfully prepared these

DOI: 10.1021/acscatal.7b03303
ACS Catal. 2018, 8, 1097−1103

multiglycidyl esters using by methyl esters and **2** without epichlorohydrin.

Studies of the transesterification of **1a** with 1 equiv of aliphatic alcohols in the presence of $(n\text{-Oct})_3$MeNCl revealed the characteristic trend of this reaction. 1-Hexanol (**4**) was not converted to hexyl benzoate (**5**) under the same conditions as for **2** (Scheme 2a). In contrast, catalytic transesterification of **1a**

Scheme 2. Transesterification with an Aliphatic Alcohol (a,b) and Methyl Carbonate Salt (c) as a Catalyst

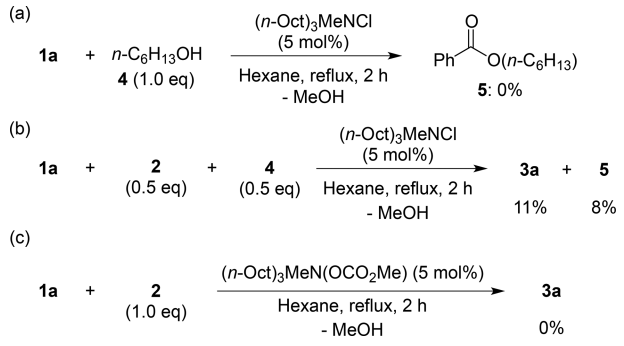

with 0.5 equiv of **2** and 0.5 equiv of **4** afforded 8% of **5** together with **3a** in 11% (Scheme 2b), indicating the involvement of **2** as the catalyst. Quaternary alkyl onium salts with methyl carbonate catalyze the transesterification of dialkyl carbonate[32] and methyl esters with aliphatic alcohols.[33] Transesterification of **1a** with **2** in the presence of 5 mol % of $(n\text{-Oct})_3$MeN(OCO_2Me),[32] however, did not afford the desired product **3a** (Scheme 2c). Thus, it is likely that the anion species derived from alkyl ammonium chloride and **2** acts as the catalyst that converts **2** to glycidyl esters in a selective manner.

To elucidate the role of quaternary alkyl ammonium salts, we recorded ^{1}H NMR of a mixture with glycidol in toluene-d_8. The ^{1}H NMR spectrum of a mixture of $(n\text{-Oct})_3$MeNCl and **2** displayed a lower magnetic-field shift of signals due to **2** and a higher magnetic-field shift of signals assignable to the $-NCH_3$ and $-NCH_2-$ groups in $(n\text{-Oct})_3$MeNCl. In fact, the binding constant (K_a) for the association between $(n\text{-Oct})_3$MeNCl and **2** in toluene-d_8 at 25 °C was $5.9 \pm 0.1 \times 10^2$ M^{-1} based on an NMR titration experiment with a 1:1 complexation nonlinear regression model (Figure 2 and S1).[35,36] Compared with the K_a of the dimerization of **2** in toluene-d_8 (1.2 ± 0.1 M^{-1}),[19] the large K_a value for the complex $[(n\text{-Oct})_3\text{MeNCl}\cdot\mathbf{2}]$ suggests that **2** in nonpolar solvent favors complexation with $(n\text{-Oct})_3$MeNCl rather than dimerization. ^{1}H–^{1}H NOESY analysis of a mixture of $(n\text{-Oct})_3$MeNCl with **2** in toluene-d_8 displayed a cross-correlation peak between all protons of **2** and $-NCH_3$ and $-NCH_2-$ (Figure S2), indicating that **2** associates around the N center of $(n\text{-Oct})_3$MeNCl. The dual interaction at the epoxide and OH group forming the dimer is known,[19] and accordingly, **2** may bind to $(n\text{-Oct})_3$MeNCl via the hydrogen bond between the OH group and the anion, forming a complex.[37] In contrast, the IR spectrum of the mixture of methyl benzoate with $(n\text{-Oct})_3$MeNCl did not show a peak shift due to a carbonyl group compared with its original spectrum in hexane (Figure S3).

Although the mixture of **2** and $(n\text{-Oct})_3$MeNCl in solution is stable at room temperature, oligomerization of **2** proceeded at a higher temperature.[38] Reaction of **2** with a catalytic amount of $(n\text{-Oct})_3$MeNCl in hexane at reflux temperature resulted in 79% consumption of **2**. On the basis of this observation and

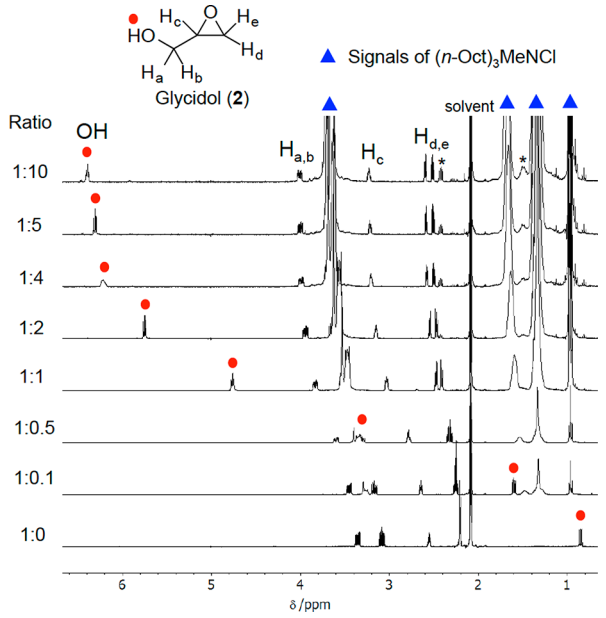

Figure 2. Titration of **2** with $(n\text{-Oct})_3$MeNCl monitored by ^{1}H NMR in toluene-d_8 (400 MHz, 25 °C). The concentration of **2** was 12 mM. A molar ratio of [**2**]:$[(n\text{-Oct})_3\text{MeNCl}]$ was varied from 1:0 to 1:10. Peaks below asterisks (*) are attributed to impurities of $[(n\text{-Oct})_3\text{MeNCl}]$.

research describing the partial ring-opening of the epoxide by ammonium salts,[39] it is considered that an alkoxide anion is generated from the complex $[(n\text{-Oct})_3\text{MeNCl}\cdot\mathbf{2}]$ through the ring-opening of the epoxide by attack of the Cl anion.

Possible mechanisms (Paths A, B, B′, B1, and B2) are depicted in Scheme 3, and the potential energy profiles for each mechanism were investigated by density functional theory computations at ωB97XD/6-311+G(d,p)//ωB97XD/6-31G(d) (Figure 3). For the calculation, $(n\text{-Bu})_4$NCl was used as a model catalyst, and *n*-hexane was incorporated as an implicit solvent (see SI for more detail). Optimized structures of the reactant, product, intermediate, and transition states are displayed in Figure S4 for Path A, Figure S5 for Paths B and B′, Figure S6 for Path B1, and Figure S7 for Path B2. First, the ammonium salt binds to glycidol, affording a precursor complex in reactant state **R**, which generates a ring-opened anion species in intermediate state **A_Int-1** through a transition state, **A_TS$_{R\text{-}1}$**. This ring-opening event goes through a high-energy barrier (E_a = 26.5 kcal/mol, **A_TS$_{R\text{-}1}$**), and the resulting intermediate state **A_Int-1** is destabilized by 8.6 kcal/mol compared with **R**. In Path A, **A_Int-1** converts to **A_Int-2** via a low activation energy transition state (E_a = 4.3 kcal/mol, **A_TS$_{1-2}$**) by intramolecular proton transfer, and **A_Int-2** could easily convert back to **A_Int-1** (E_a = 2.7 kcal/mol, **A_TS$_{1-2}$**), which means that this step is an equilibrium process. After this step, methyl ester addition occurs (**A_Int-3**) and nucleophilic attack of the alkoxide species in the **A_Int-3** state on a carbonyl group of methyl ester gives the intermediate state **A_Int-4**. The energy barrier of the C–O bond formation (E_a = 7.1 kcal/mol, **A_TS$_{3-4}$**) is lower than that of **A-TS$_{R\text{-}1}$** (E_a = 26.5 kcal/mol), indicating that C–O bond formation is not the rate-determining step in Path A. After the dissociation of methanol (MeOH), the ring-closing reaction in the **A_Int-5** state produces the glycidyl ester and regenerates the $(n\text{-Bu})_4$NCl, and the catalytic cycle returns to the reactant state **R**. In Path A,

DOI: 10.1021/acscatal.7b03303
ACS Catal. 2018, 8, 1097–1103

Scheme 3. Possible Mechanism for Catalytic Transesterification by Glycidol[a]

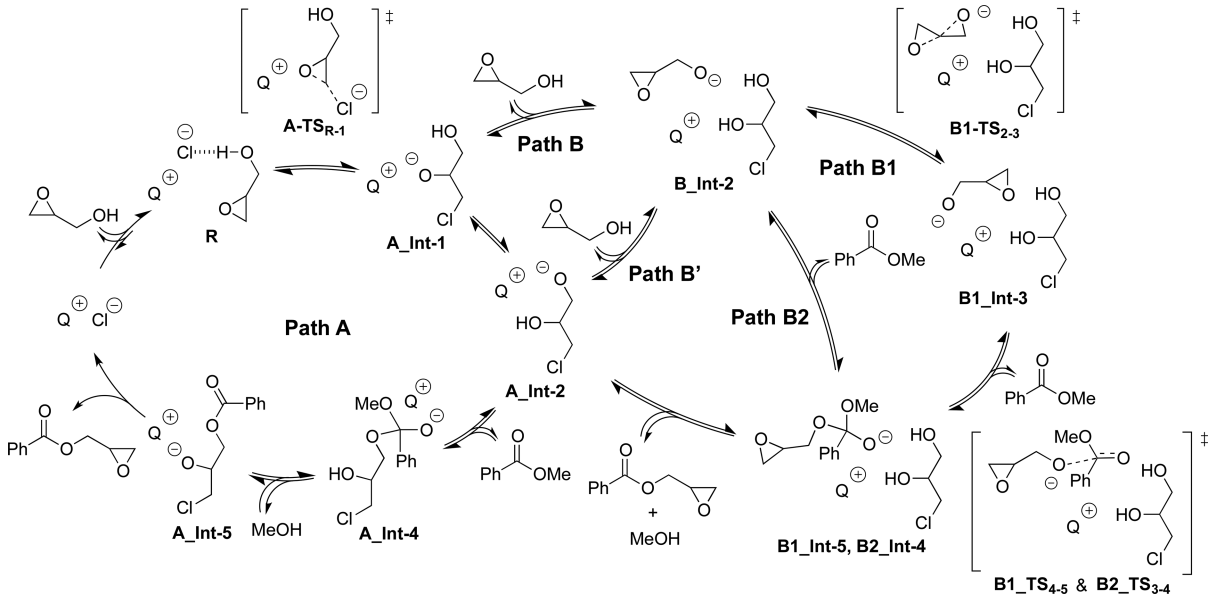

[a]Q represents $(n\text{-Bu})_4$N.

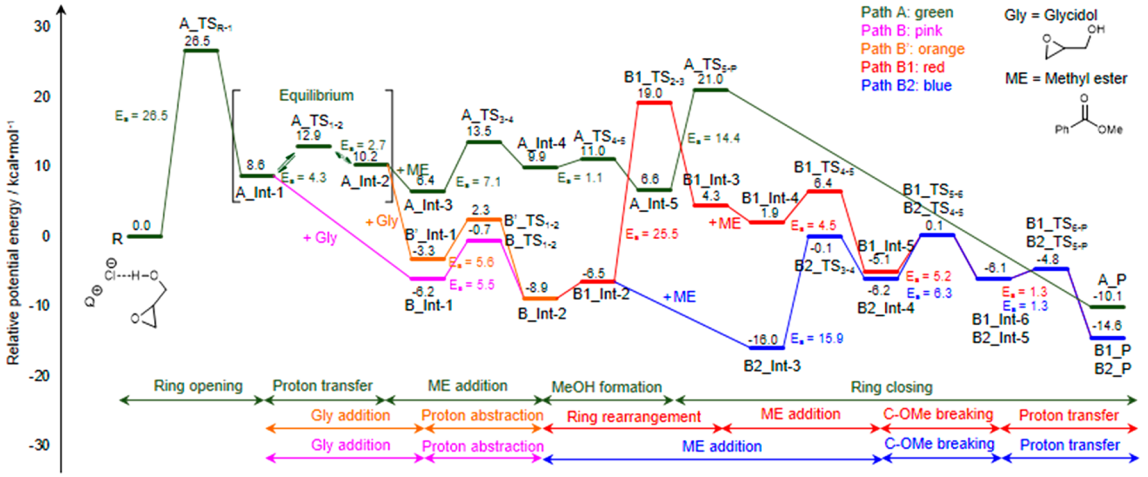

Figure 3. Potential energy profiles for the synthesis of glycidyl esters from methyl ester with glycidol which catalyzed by $(n\text{-Bu})_4$NCl.

the reaction must overcome a high-energy barrier of 26.5 kcal/mol at the ring-opening step of **2** in every catalytic cycle.

Alternatively, ring-opened intermediate states **A_Int-1** and **A_Int-2** can initiate other catalytic cycles. The addition of glycidol to **A_Int-1** and **A_Int-2** can generate different pathways, Paths B and B′, respectively. These two pathways include proton abstraction from glycidol, and the alkoxide species in the **A_Int-1** and **A_Int-2** states are structural isomers of each other. The B and B′ pathways reach a common intermediate state, **B_Int-2**, because of their structural similarity. The calculated activation energy for the proton abstraction in Paths B and B′ was 5.5 kcal/mol (**B_TS$_{1-2}$**) and 5.6 kcal/mol (**B′_TS$_{1-2}$**), respectively.

The alkoxide species in intermediate state **B_Int-2** works as the active species of the nucleophilic addition to methyl ester. Here, we considered two pathways; the first one (Path B1) involves isomerization of the alkoxide species via the Payne rearrangement,[40] followed by nucleophilic addition to methyl ester. The second pathway (Path B2) directly proceeds to the nucleophilic addition to methyl ester.

In Path B1, the rate-determining step is the Payne rearrangement. The calculated activation energy was 25.5 kcal/mol (**B1_TS$_{2-3}$**). Because this rearrangement is a ring-opening step of the epoxide, the amount of E_a is similar to that of the ring-opening transition state (**A_TS$_{R-1}$**). The transition state of the Payne rearrangement (**B1_TS$_{2-3}$**) is energetically unfavorable, due to the double hydrogen bonds between the alkoxide anion and diol in **B1_Int-2**.[41] The resulting anion species **B1_Int-3** is also less unstable by 10.8 kcal/mol compared with **B1_Int-2**, even though the alkoxide anion interacts with positively charged H atoms in the ammonium cation.[42] Due to this destabilized form, the attack of the alkoxide anion on the carbonyl group is a low-energy barrier process (E_a = 4.5 kcal/mol, **B1_TS$_{4-5}$**). After methyl ester addition, the C-OMe breaking (E_a = 5.2 kcal/mol, **B1_TS$_{5-6}$**) is followed by proton transfer steps (E_a = 1.3 kcal/mol, **B1_TS$_{6-P}$**). The product state from transition state **B1_TS$_{6-P}$** involves alkoxide species that are the same as in **A_Int-2**. Therefore, the next catalytic cycle enters Path B′ directly or Path B via **A_Int-1**. We note that the reaction process can enter

DOI: 10.1021/acscatal.7b03303
ACS Catal. 2018, 8, 1097−1103

Path A from **A_Int-2**. As mentioned above, however, this process is energetically unfavorable, because Path A has to go through the ring-opening transition state **A_TS$_{R-1}$** (E_a = 26.5 kcal/mol).

In Path B2, the highest energy barrier process is the nucleophilic addition of alkoxide species (E_a = 15.9 kcal/mol, **B2_TS$_{3-4}$**). This result is consistent with the fact that substrates having an electron-withdrawing group were efficiently converted to the desired products (Table 1). Compared with the rate-determining step in Path B1 (Payne rearrangement), the calculated activation energy of Path B2 is lower by 9.6 kcal/mol. From the intermediates **B2_Int-4**, the C-OMe breaking through **B2_TS$_{4-5}$** (E_a = 6.3 kcal/mol) is followed by a proton transfer (E_a = 1.3 kcal/mol, **B2_TS$_{5-P}$**) to reach the product state. The catalytic process returns to **A_Int-2** and reaches **B_Int-2** via Path B or Path B′.

Several intermediate states allow glycidol to enter the polymerization process. These polymerization pathways are energetically unfavorable, however, because a ring-opening process is involved. Intermediate states **A_Int-1**, **B_Int-2**, and **B1_Int-3** occur just before nucleophilic addition to methyl ester, and therefore alkoxide species are available. If these active species attack another glycidol, dimerization is initiated. As shown in Figure S8, the calculated activation energies for dimerization from **A_Int-1**, **B_Int-2**, and **B1_Int-3** are 22.1, 25.2, and 14.0 kcal/mol, respectively. In the first two cases, the barrier height is as high as the other ring-opening steps (E_a = 26.5 and 25.5 kcal/mol for **A_TS$_{R-1}$** and **B1_TS$_{2-3}$**, respectively). In the third case, because of the instability of the **B1_Int-3** state, the calculated activation energy was lower than that of the other ring-opening steps. Once the **B1_Int-3** state thermally relaxes into a more stable conformation, such as the **B_Int-2** state, the activation energy becomes much higher. In any case, access to the **B1_Int-3** state is inhibited by the energy barrier of the Payne rearrangement.

As the energy barrier of ring-opening reactions of epoxide is relatively high, Path B2 is the most favorable pathway for transesterification. This result also indicates that the alkyl ammonium cation has less of an effect to promote the ring-opening step than the system with Lewis acid,[42a] which inhibits the random ring-opening reaction and polymerization.

CONCLUSION

In conclusion, we demonstrated the effective transformation of glycidol to valuable compounds while the epoxide part remains intact. The unexpected involvement of glycidol as a catalyst with the alkyl ammonium salt was elucidated experimentally as well as computationally. The minimal interaction of the alkyl ammonium cation with epoxide inhibited the undesired ring-opening polymerization, and enabled the controlled transformation of glycidol. This finding may provide an alternative strategy for synthesizing functional compounds and materials containing epoxy moieties, including those derivatized from epoxy compounds, because a glycidyl group could be installed not by the electrophilic reaction of epichlorohydrin, but by the nucleophilic reaction of glycidol. Further studies of the detailed mechanisms of alkoxide anion generation by onium salt, and optimization of cation−anion combinations are underway in our laboratory.

EXPERIMENTAL SECTION

General Procedure. ^{1}H NMR (400 MHz) and ^{13}C{^{1}H} NMR (100 MHz) spectra were recorded on JEOL 400 MHz NMR spectrometers. All spectra were recorded at 25 ± 1 °C. Chemical shifts (δ) are in parts per million relative to tetramethylsilane at 0 ppm for ^{1}H, and $CDCl_3$ at 77.0 ppm for ^{13}C unless otherwise noted. IR spectra were recorded on Mettler Toledo ReactIR-4000. Gas chromatographic (GC) analyses were performed on a Shimadzu GC-2014 using a TC-1 column (0.25 mm × 30 m, GL Sciences Inc.). All samples were analyzed and quantified by using biphenyl as an internal standard. $(n\text{-Oct})_3MeN(OCO_2Me)$ was synthesized by the reported procedure.[34] Other chemicals were purchased from chemical suppliers. Glycidol was distilled under an atmospheric pressure before to use in order to remove oligomers. Other chemicals were used as received. Catalytic reactions were performed using ChemiStation (Tokyo Rika Inc.) equipped with thermostated apparatus.

Procedure for Catalytic Reaction. To a solution of catalyst (0.050 mmol) in hexane (0.5 mL), methyl ester (1.0 mmol) and glycidol (1.0 mmol) were added. After stirring 2 h at reflux temperature (69 °C), reaction mixture was diluted with CH_3CN (3 mL) and filtered. Extra CH_3CN (3 mL × 2) was used for a collection of residual chemicals in a test tube, and this solution was also filtered. To a combined solution was then added measured amount of biphenyl (as an internal standard for NMR analysis), and an aliquot was used for NMR measurement. The conversion of substrate and the yield of products were determined by ^{1}H NMR analysis (400 MHz, $CDCl_3$, 25 °C). GC-FID of same solution was measured for the determination of conversion of glycidol. For the isolation of glycidyl esters, silica-gel column chromatography was carried out using EtOAc and hexane as eluent.

COMPUTATIONAL DETAILS

All the computations were done with Gaussian 09.[43] Density functional theory (DFT) calculations at the ωB97XD[44]/6-31G* level were carried out for the structure optimization. In order to obtain accurate potential energies, single-point calculations were computed at the ωB97XD/6-311+G** level. According to a previous assessment[45] on the applicability of the dispersion corrected DFT to the molecular interactions, ωB97XD performed best among the 18 functionals including M06-2X and LC-BOP-LRD. The solvation effect was included with the self-consistent reaction field (SCRF) method, and the dielectric constant of *n*-hexane was used.[46] Natural population analysis (NPA) was performed with NBO ver 3.1 in the Gaussian package.[47] The transition-state structures were verified by frequency calculations.

For the consistency of the potential energy profile in Figure 3, energy of glycidol and methyl ester were added to those of the reactant states, transition states, and intermediate states. For example, energy of glycidol and methyl ester were added to those of R, A_TS$_{R-1}$, A_Int-1, A_TS$_{1-2}$, A_Int-2 in Path A. In calculating the energies of glycidol and methyl ester in their isolated states, explicit interactions with solvent molecule S (S = *n*-hexane) have to be taken into account because the continuum model cannot describe the explicit hydrogen bonding energy and CH-π interaction. Otherwise, such interactions were taken into account only in the complex. We adopted an energy correction for X (X = glycidol or methyl ester) such as E_int = E(X+S) − E(X) − E(S). The E_int value for glycidol was 4.0

DOI: 10.1021/acscatal.7b03303
ACS Catal. 2018, 8, 1097−1103

kcal/mol, which represents hydrogen bonding. The E_int value for methyl ester was 8.0 kcal/mol, which represents both hydrogen bonding and CH−π interactions.

■ ASSOCIATED CONTENT

Supporting Information

The Supporting Information is available free of charge on the ACS Publications website at DOI: 10.1021/acscatal.7b03303.

Study on reaction condition of catalytic transesterification (Table S1); determination of equilibrium constants by ^{1}H NMR (Table S2, Figure S1); observation of glycidol, substrate, and quaternary alkyl ammonium salts in solution (Figures S2, S3); optimized structures in computational study (Figure S4−S8); and characterization of isolated products (PDF)

■ AUTHOR INFORMATION

Corresponding Authors

*E-mail for S.T.: shinji-tanaka@aist.go.jp.
*E-mail for J.H.: hasegawa@cat.hokudai.ac.jp.
*E-mail for K.S.: k.sato@asit.go.jp.

ORCID

Shinji Tanaka: 0000-0003-2002-5582
Jun-ya Hasegawa: 0000-0002-9700-3309

Notes

The authors declare no competing financial interest.

■ ACKNOWLEDGMENTS

We thank Prof. Dr. Hirose (Osaka University) for his advice on a NMR titration experiment. S.T. acknowledges financial support by Grant-in-Aid for Scientific Research on Innovative Areas (JSPS KAKENHI Grant No. JP16H01044 in Precisely Designed Catalysts with Customized Scaffolding). J.H. also appreciates financial support from the same area (No. JP15H05805). A part of the calculations was performed using Research Center for Computational Science, Okazaki, Japan.

■ REFERENCES

(1) Oki, M.; Murayama, T. *Bull. Chem. Soc. Jpn.* **1973**, *46*, 259−263.
(2) (a) Marstokk, K.-M.; Møllendal, H.; Stenstrøm, Y. *Acta Chem. Scand.* **1992**, *46*, 432−441. (b) Marstokk, K.-M.; Møllendal, H.; Samdal, S.; Stenstrøm, Y. *Acta Chem. Scand.* **1992**, *46*, 325−337.
(3) Becucci, M.; Melandri, S. *Chem. Rev.* **2016**, *116*, 5014−5037.
(4) Demaison, J.; Craig, N. C.; Conrad, A. R.; Tubergen, M. J.; Rudolph, H. D. *J. Phys. Chem. A* **2012**, *116*, 9116−9122.
(5) Maris, A.; Giuliano, B. M.; Bonazzi, D.; Caminati, W. *J. Am. Chem. Soc.* **2008**, *130*, 13860−13861.
(6) Hanson, R. M. *Chem. Rev.* **1991**, *91*, 437−478.
(7) (a) Leal-Duaso, A.; Caballero, M.; Urriolabeitia, A.; Mayoral, J. A.; García, J. I.; Pires, E. *Green Chem.* **2017**, *19*, 4176−4185. (b) Cucciniello, R.; Ricciardi, M.; Vitiello, R.; Di Serio, M.; Proto, A.; Capacchione, C. *ChemSusChem* **2016**, *9*, 3272−3275. (c) Ricciardi, M.; Passarini, F.; Vassura, I.; Proto, A.; Capacchione, C.; Cucciniello, R.; Cespi, D. *ChemSusChem* **2017**, *10*, 2291−2300.
(8) (a) Cespi, D.; Cucciniello, R.; Ricciardi, M.; Capacchione, C.; Vassura, I.; Passarini, F.; Proto, A. *Green Chem.* **2016**, *18*, 4559−4570. (b) Kondawar, S. E.; Patil, C. R.; Rode, C. V. *ACS Sustainable Chem. Eng.* **2017**, *5*, 1763−1774.
(9) Wang, C.; Luo, L.; Yamamoto, H. *Acc. Chem. Res.* **2016**, *49*, 193−204.
(10) Wilms, D.; Stiriba, S.-E.; Frey, H. *Acc. Chem. Res.* **2010**, *43*, 129−141.
(11) Sandler, S. R.; Berg, F. R. *J. Polym. Sci., Part A-1: Polym. Chem.* **1966**, *4*, 1253−1259.
(12) Tsuruta, T.; Inoue, S.; Koenuma, H. *Makromol. Chem.* **1968**, *112*, 58−65.
(13) Vandenberg, E. J. *J. Polym. Sci., Polym. Chem. Ed.* **1985**, *23*, 915−949.
(14) Leibig, D.; Seiwert, J.; Liermann, J. C.; Frey, H. *Macromolecules* **2016**, *49*, 7767−7776.
(15) Goodwin, A.; Baskaran, D. *Macromolecules* **2012**, *45*, 9657−9665.
(16) Haag, R.; Sunder, A.; Stumbe, J.-F. *J. Am. Chem. Soc.* **2000**, *122*, 2954−2955.
(17) Pascault, J. P., Williams, R. J. In *Epoxy Polymers: New Materials and Innovations*; Pascault, J. P., Williams, R. J. J., Eds.; Wiley-VCH: Weinheim, Germany, 2010; pp 1−12.
(18) Auvergne, R.; Caillol, S.; David, G.; Boutevin, B.; Pascault, J.-P. *Chem. Rev.* **2014**, *114*, 1082−1115.
(19) Della Monica, F.; Buonerba, A.; Grassi, A.; Capacchione, C.; Milione, S. *ChemSusChem* **2016**, *9*, 3457−3464.
(20) Reactions of glycidol with an unsaturated bond catalyzed by tin salts accompany the ring opening reactions. See examples: (a) Edwards, P. A.; Striemer, G.; Webster, D. C. *Prog. Org. Coat.* **2006**, *57*, 128−139. (b) Edwards, P. A.; Striemer, G.; Webster, D. C. *J. Coat. Technol. Res.* **2005**, *2*, 517−527. (c) Chattopadhyay, D. K.; Zakula, A. D.; Webster, D. C. *Prog. Org. Coat.* **2009**, *64*, 128−137. (d) Pitet, L. M.; Hait, S. B.; Lanyk, T. J.; Knauss, D. M. *Macromolecules* **2007**, *40*, 2327−2334.
(21) (a) McClure, D. E.; Engelhardt, E. L.; Mensler, K.; King, S.; Saari, W. S.; Huff, J. R.; Baldwin, J. J. *J. Org. Chem.* **1979**, *44*, 1826−1831. (b) Morgan, T. K., Jr.; Lis, R.; Lumma, W. C., Jr.; Wohl, R. A.; Nickisch, K.; Phillips, G. B.; Lind, J. M.; Lampe, J. W.; Di Meo, S. V. *J. Med. Chem.* **1990**, *33*, 1087−1090.
(22) Saburi, H.; Tanaka, S.; Kitamura, M. *Angew. Chem., Int. Ed.* **2005**, *44*, 1730−1732.
(23) Deng, J.; Liu, X.; Li, C.; Jiang, Y.; Zhu, J. *RSC Adv.* **2015**, *5*, 15930−15939.
(24) Coish, P.; Brooks, B. W.; Gallagher, E. P.; Kavanagh, T. J.; Voutchkova-Kostal, A.; Zimmerman, J. B.; Anastas, P. T. *ACS Sustainable Chem. Eng.* **2016**, *4*, 5900−5906.
(25) Zondler, H.; Trachsler, D.; Lohse, F. *Helv. Chim. Acta* **1977**, *60*, 1845−1860.
(26) Degussa Aktiengesellschaft. U.S. Patent No. US4667044A, 1987.
(27) Shah, P. N.; Kim, N.; Huang, Z.; Jayamanna, M.; Kokil, A.; Pine, A.; Kaltsas, J.; Jahngen, E.; Ryan, D. K.; Yoon, S.; Kovar, R. F.; Lee, Y. *RSC Adv.* **2015**, *5*, 38673−38679.
(28) Otera, J. *Chem. Rev.* **1993**, *93*, 1449−1470.
(29) Hatano, M.; Ishihara, K. *Chem. Commun.* **2013**, *49*, 1983−1997.
(30) (a) Nakatake, D.; Yazaki, R.; Ohshima, T. *Eur. J. Org. Chem.* **2016**, *2016*, 3696−3699. (b) Nakatake, D.; Yokote, Y.; Matsushima, Y.; Yazaki, R.; Ohshima, T. *Green Chem.* **2016**, *18*, 1524−1530. (c) Horikawa, R.; Fujimoto, C.; Yazaki, R.; Ohshima, T. *Chem. - Eur. J.* **2016**, *22*, 12278−12281. (d) Agura, K.; Hayashi, Y.; Wada, M.; Nakatake, D.; Mashima, K.; Ohshima, T. *Chem. - Asian J.* **2016**, *11*, 1548−1554. (e) Mashima, K.; Hayashi, Y.; Agura, K.; Ohshima, T. *Pure Appl. Chem.* **2014**, *86*, 335−343. (f) Hayashi, Y.; Santoro, S.; Azuma, Y.; Himo, F.; Ohshima, T.; Mashima, K. *J. Am. Chem. Soc.* **2013**, *135*, 6192−6199.
(31) A study on reaction conditions such as solvent, temperature, amount of **2** and catalyst is summarized in Table S1 in Supporting Information.
(32) (a) Selva, M.; Noè, M.; Perosa, A.; Gottardo, M. *Org. Biomol. Chem.* **2012**, *10*, 6569−6578. (b) Selva, M.; Caretto, A.; Noè, M.; Perosa, A. *Org. Biomol. Chem.* **2014**, *12*, 4143−4155.
(33) Yoshida, Y.; Ogura, Y.; Hatano, M.; Ishihara, K. Presented at the 96th Chemical Society of Japan Annual Meeting, Kyoto, Japan, Mar. 24−27, 2016.
(34) Fabris, M.; Lucchini, V.; Noè, M.; Perosa, A.; Selva, M. *Chem. - Eur. J.* **2009**, *15*, 12273−12282.
(35) Hirose, K. *J. Inclusion Phenom. Mol. Recognit. Chem.* **2001**, *39*, 193−209.
(36) Thordarson, P. *Chem. Soc. Rev.* **2011**, *40*, 1305−1323.

DOI: 10.1021/acscatal.7b03303
ACS Catal. 2018, 8, 1097−1103

(37) An interaction of halogen anion of quaternary alkyl onium salts with OH group was proposed in some literatures. See examples: (a) Liu, S.; Suematsu, N.; Maruoka, K.; Shirakawa, S. *Green Chem.* **2016**, *18*, 4611−4615. (b) Kondo, S.; Okada, N.; Tanaka, R.; Yamamura, M.; Unno, M. *Tetrahedron Lett.* **2009**, *50*, 2754−2757. (c) Ito, K.; Nishiki, M.; Ohba, Y. *Chem. Pharm. Bull.* **2005**, *53*, 1352−1354.
(38) Attempts to observe the ring-opened products were unsuccessful. ^{1}H NMR of mixture of $(n\text{-Oct})_3$MeNCl with **2** in toluene-d_8 showed only signals due to oligomers of **2** after heating up to 50 °C
(39) (a) Buddrus, J. *Angew. Chem., Int. Ed. Engl.* **1972**, *11*, 1041−1110. (b) Font, J.; Galán, M. A.; Virgili, A. *J. Chem. Soc., Perkin Trans. 2* **1986**, 75−78.
(40) Payne, G. B. *J. Org. Chem.* **1962**, *27*, 3819−3822.
(41) Dua, S.; Taylor, M. S.; Buntine, M. A.; Bowie, J. H. *J. Chem. Soc., Perkin Trans. 2* **1997**, 1991−1997.
(42) (a) Ema, T.; Miyazaki, Y.; Shimonishi, J.; Maeda, C.; Hasegawa, J. *J. Am. Chem. Soc.* **2014**, *136*, 15270−15279. (b) Ema, T.; Fukuhara, K.; Sakai, T.; Ohbo, M.; Bai, F.-Q.; Hasegawa, J. *Catal. Sci. Technol.* **2015**, *5*, 2314−2321.
(43) Frisch, M. J.; Trucks, G. W.; Schlegel, H. B.; Scuseria, G. E.; Robb, M. A.; Cheeseman, J. R.; Scalmani, G.; Barone, V.; Mennucci, B.; Petersson, G. A.; Nakatsuji, H.; Caricato, M.; Li, X.; Hratchian, H. P.; Izmaylov, A. F.; Bloino, J.; Zheng, G.; Sonnenberg, J. L.; Hada, M.; Ehara, M.; Toyota, K.; Fukuda, R.; Hasegawa, J.; Ishida, M.; Nakajima, T.; Honda, Y.; Kitao, O.; Nakai, H.; Vreven, T.; Montgomery, Jr., J. A.; Peralta, J. E.; Ogliaro, F.; Bearpark, M.; Heyd, J. J.; Brothers, E.; Kudin, K. N.; Staroverov, V. N.; Kobayashi, R.; Normand, J.; Raghavachari, K.; Rendell, A.; Burant, J. C.; Iyengar, S. S.; Tomasi, J.; Cossi, M.; Rega, N.; Millam, J. M.; Klene, M.; Knox, J. E.; Cross, J. B.; Bakken, V.; Adamo, C.; Jaramillo, J.; Gomperts, R.; Stratmann, R. E.; Yazyev, O.; Austin, A. J.; Cammi, R.; Pomelli, C.; Ochterski, J. W.; Martin, R. L.; Morokuma, K.; Zakrzewski, V. G.; Voth, G. A.; Salvador, P.; Dannenberg, J. J.; Dapprich, S.; Daniels, A. D.; Farkas, Ö.; Foresman, J. B.; Ortiz, J. V.; Cioslowski, J.; Fox, D. J. *Gaussian 09, revision D.01*; Gaussian, Inc.: Wallingford, CT, 2009.
(44) Chai, J.-D.; Head-Gordon, M. *Phys. Chem. Chem. Phys.* **2008**, *10*, 6615−6620.
(45) Grimme, S. *WIREs Computational Molecular Science* **2011**, *1*, 211−228.
(46) (a) Miertuš, S.; Scrocco, E.; Tomasi, J. *Chem. Phys.* **1981**, *55*, 117−129. (b) Mennucci, B.; Tomasi, J. *J. Chem. Phys.* **1997**, *106*, 5151−5158. (c) Cammi, R.; Mennucci, B.; Tomasi, J. *J. Phys. Chem. A* **2000**, *104*, 5631−5638.
(47) (a) Reed, A. E.; Weinhold, F. *J. Chem. Phys.* **1983**, *78*, 4066−4073. (b) Reed, A. E.; Weinstock, R. B.; Weinhold, F. *J. Chem. Phys.* **1985**, *83*, 735−746.

DOI: 10.1021/acscatal.7b03303
ACS Catal. 2018, 8, 1097−1103